

Supplementary Materials for
**Chronic exposure to glucocorticoids amplifies inhibitory neuron cell fate
during human neurodevelopment in organoids**

Leander Dony *et al.*

Corresponding author: Elisabeth B. Binder, binder@psych.mpg.de; Cristiana Cruceanu, cristiana.cruceanu@ki.se

Sci. Adv. **11**, eadn8631 (2025)
DOI: 10.1126/sciadv.adn8631

The PDF file includes:

Figs. S1 to S6
Legends for tables S1 to S9

Other Supplementary Material for this manuscript includes the following:

Tables S1 to S9

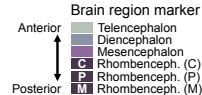
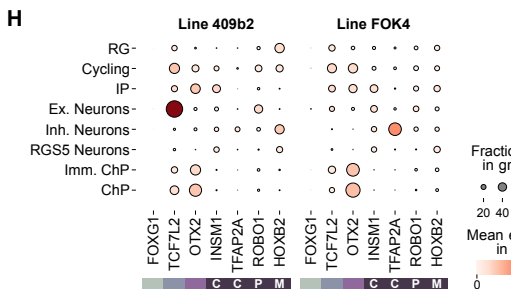
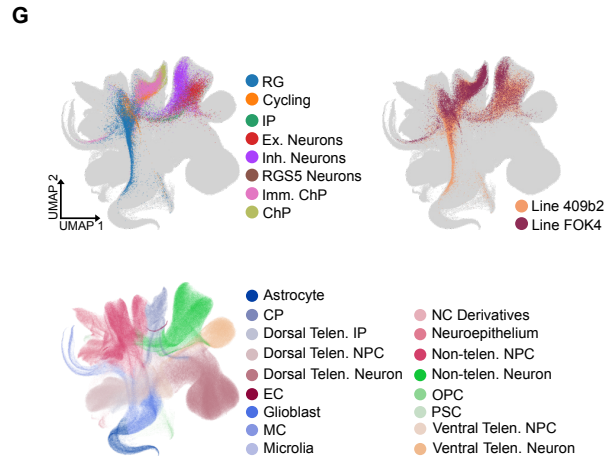
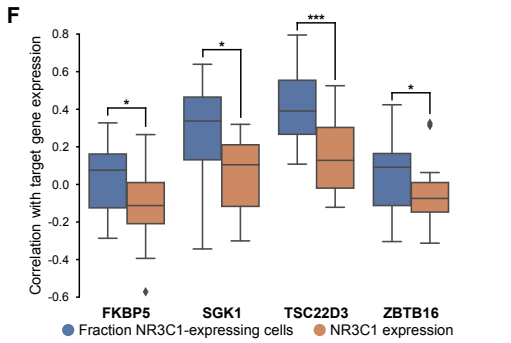
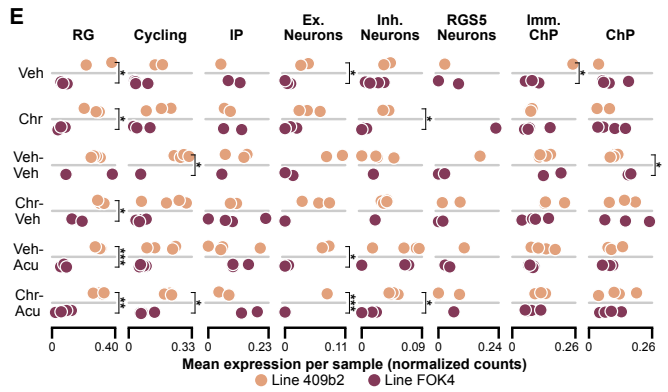
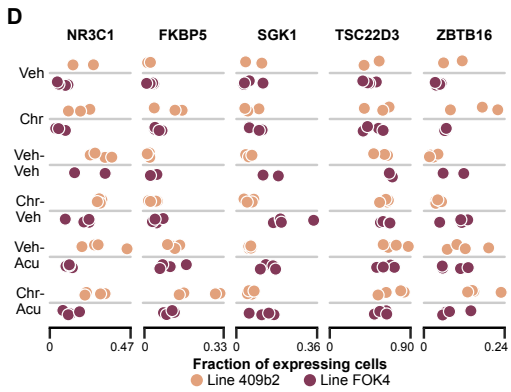
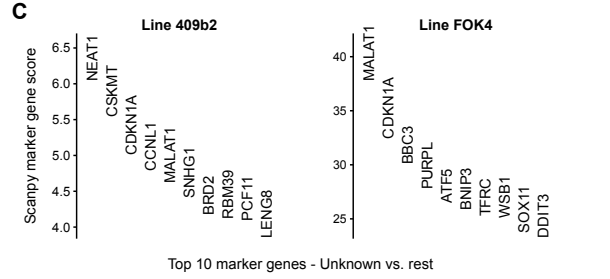
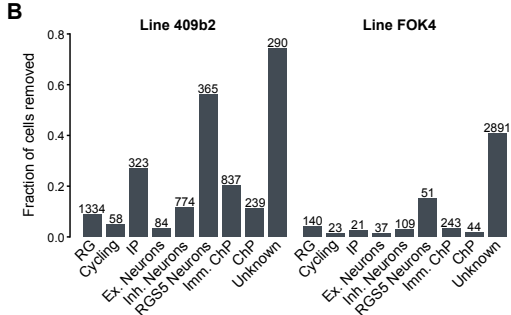
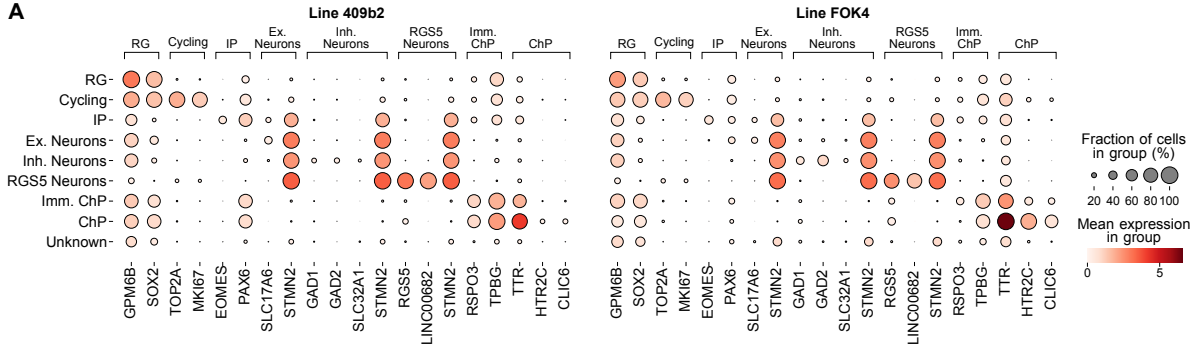


Fig. S1: Chronic glucocorticoid exposure in neural organoids does not induce significant metabolic stress in cells. (A) Selected marker gene expression per cell type and cell line. (B) Fraction of non-viable cells per cell type and cell line. The absolute number of non-viable cells per cluster is displayed above each bar. The “Unknown” clusters were removed from the datasets in their entirety (394 cells in Line 409b2; 7039 cells in Line FOK4). (C) Top 10 marker genes of the remaining cells from the Unknown cluster after viability score-based removal of cells. (D) Fraction of expressing cells per sample across two cell lines and six conditions for *NR3C1* and four canonical GC-responsive genes. No significant differences were found between cell lines after multiple testing correction using an unpaired t-test. (E) *NR3C1* expression levels per cell type and treatment condition, considering celltype/samples with more than 10 cells. Significant FDR-corrected p-values (unpaired t-test): RG Veh 0.047, RG Chr 0.0056, RG Chr-Veh 0.0056, RG Veh-Acu 0.000027, RG Chr-Acu 0.0020, Cycling Veh-Veh 0.036, Cycling Chr-Acu 0.016, Ex.Neurons Veh 0.020, Ex.Neurons Veh-Acu 0.0060, Ex.Neurons Chr-Acu 0.00, Inh.Neurons Chr 0.0056, Inh.Neurons Chr-Acu 0.017, Imm.ChP Veh 0.028, ChP Veh-Veh 0.020. (F) Correlation between the fraction of *NR3C1*-expressing cells (blue) or *NR3C1* expression level (maroon) and expression level of *NR3C1*-target genes in the cell types with cell line specific *NR3C1* expression differences (RG, Cycling, Ex. and Inh. Neurons, Imm. ChP, and ChP). Significant FDR-corrected p-values (paired t-test): FKBP5 0.0055, SGK1 0.0055, TSC22D3 0.00049, ZBTB16 0.038. (G) Top: cells from this publication projected to the HNOCA(36). Cells are colored by their origin dataset (left) and cell types assigned in this study (right). Bottom: HNOCA cell type labels. CP, choroid plexus; NPC, neural progenitor cell; EC, endothelial cell; MC, mesenchymal cell; NC, neural crest; OPC, oligodendrocyte progenitor cell; PSC, pluripotent stem cell. (H) Selected regional anterior to posterior marker gene expression per cell type and cell line. C, Cerebellum; P, Pons; M, Medulla.

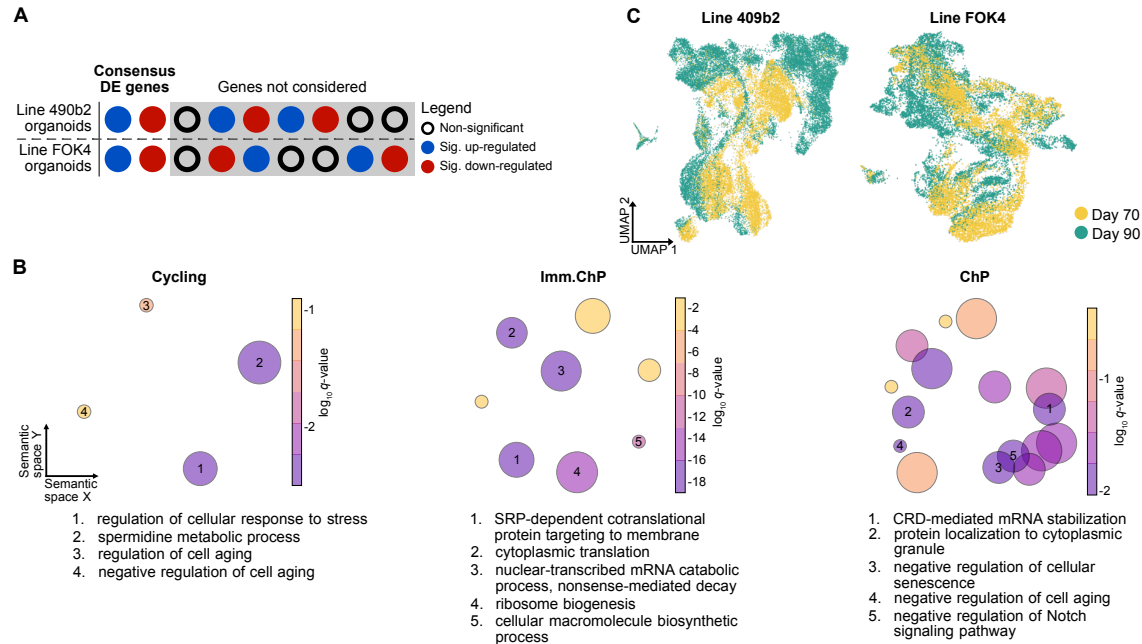


Fig. S2: Transcriptional response following chronic glucocorticoid treatment in organoids includes key neurodevelopmental genes. (A) Filtering scheme used to identify consensus DE genes between organoids from the two genetic backgrounds. (B) Grouped semantic space representation of the GO-BP enrichment analysis for the three cell types with the least detected DE genes. The size of the circles corresponds to the number of terms in the cluster; their color corresponds to the $\log_{10}(\text{q-value})$ of the representative term for each cluster. The integers within the circles enumerate the five most significant clusters, and their representative term is written out in the legend below each plot. (C) UMAP embedding of Line 409b2 and Line FOK4 data colored by organoid age.

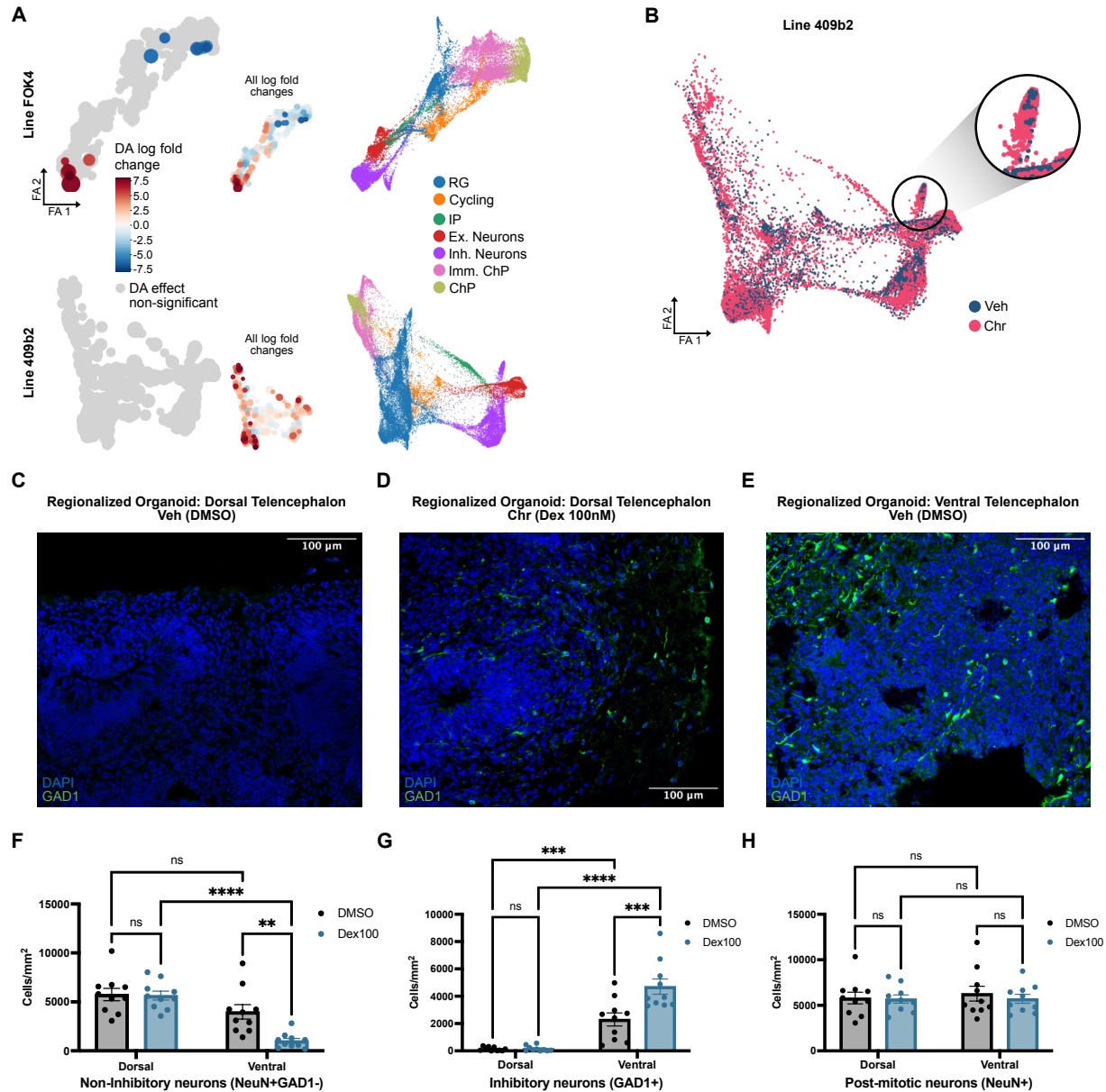


Fig. S3: GC exposure results in an increased abundance of inhibitory neurons in organoids.

(A) Milo(45) differential accessibility (DA) results per neighborhood ($k=30$). Left: log fold-changes of significantly differentially accessible neighborhoods (red = increased in Chr, blue = decreased in Chr); Middle: DA log fold-changes of all neighborhoods; Right: cell type assignments on force-directed graph layout. Top: Line FOK4, Bottom: Line 409b2. FA, force-directed graph embedding. (B) Line 409b2 force-directed graph layout colored by treatment. The magnified area of the embedding corresponds to the relevant subset of inhibitory neurons with high GAD1 expression. (C) Representative image of whole slice dorsalized Line 409b2 (GFP-*GAD1*) control organoids at day 70 in culture (Veh condition). Only very few GAD1+ cells are visible. DMSO, dimethyl sulfoxide; Dex, dexamethasone. (D) Representative image of whole slice dorsalized Line 409b2 (GFP-*GAD1*) organoids at day 70 in culture, following 10 days of chronic treatment with GCs (100nM dexamethasone; Chr condition). Only very few GAD1+ cells are visible, but slightly more than in the dorsalized control organoids. (E) Representative

image of whole slice ventralized Line 409b2 (GFP-GAD1) control organoids at day 70 in culture (Veh condition). A larger number of GAD1+ cells as compared to the dorsalized organoids indicates a successful ventralization. Statistical significance was computed using an unpaired t-test. **(F)** Immunofluorescence-based non-inhibitory neuron (NeuN+GAD1- cells) quantification in both ventralized and dorsalized organoids. Statistical significance was computed using an unpaired t-test. **(G)** Immunofluorescence-based Inhibitory neuron (GAD1+ cells) quantification in both ventralized and dorsalized organoids. **(H)** Immunofluorescence-based post-mitotic neuron (NeuN+ cells) quantification in both ventralized and dorsalized organoids. Statistical significance was computed using an unpaired t-test.

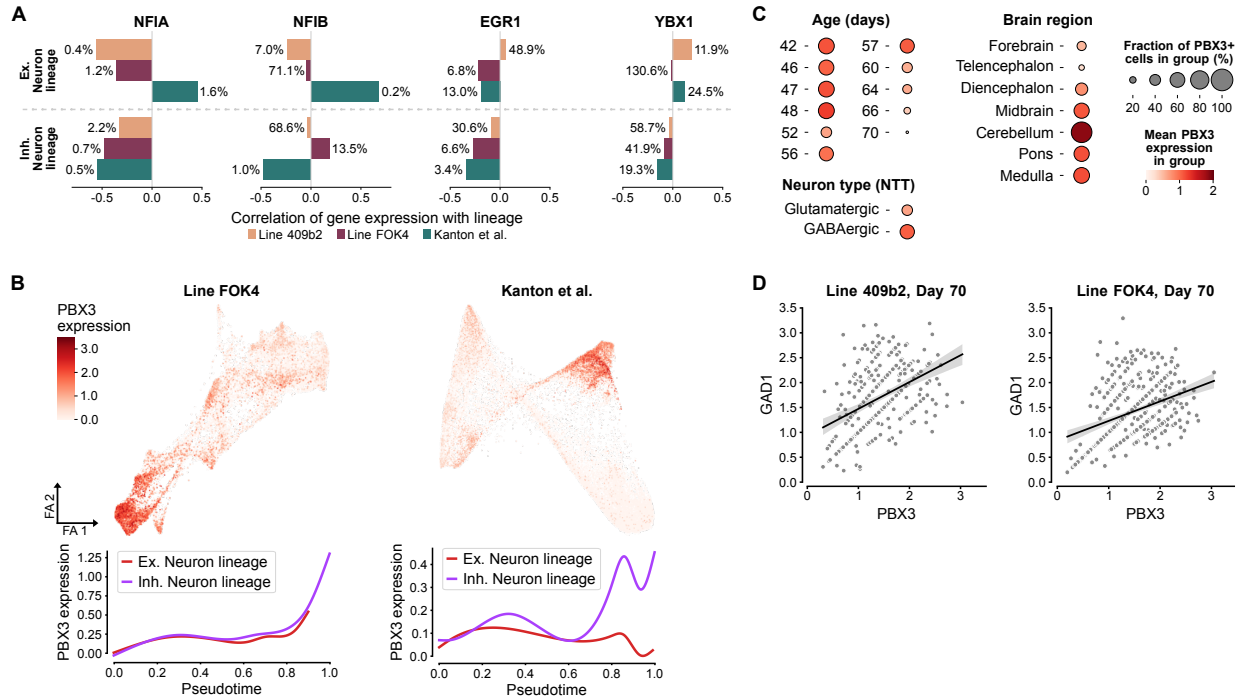


Fig. S4: PBX3 regulation through chronic glucocorticoid exposure supports inhibitory neuron priming. (A) Correlation of *NFIA*, *NFIB*, *YBX1*, and *EGR1* expression with lineage probability across the excitatory and inhibitory neuronal lineages in all three datasets. The percentile of each gene among all significant driver genes ranked by driver strength is shown on the side of every bar. (B) Top: Expression of *PBX3* in Line FOK4 and the validation data (Kanton et al.) on a force-directed graph embedding. Bottom: Expression patterns of *PBX3* across pseudotime for each of the three lineage endpoints in Line FOK4 and the validation data (Kanton et al.). FA, force-directed graph embedding. (C) Expression of *PBX3* in the fetal brain atlas(48) neurons and progenitors across age (in days), dissected brain region, and neurotransmitter-transporter expression (left to right). NTT, neurotransmitter transporter (D) Expression of *GAD1* and *PBX3* in day-70 double-positive cells with fitted linear regression line. Left: Line 409b2. Right: Line FOK4.

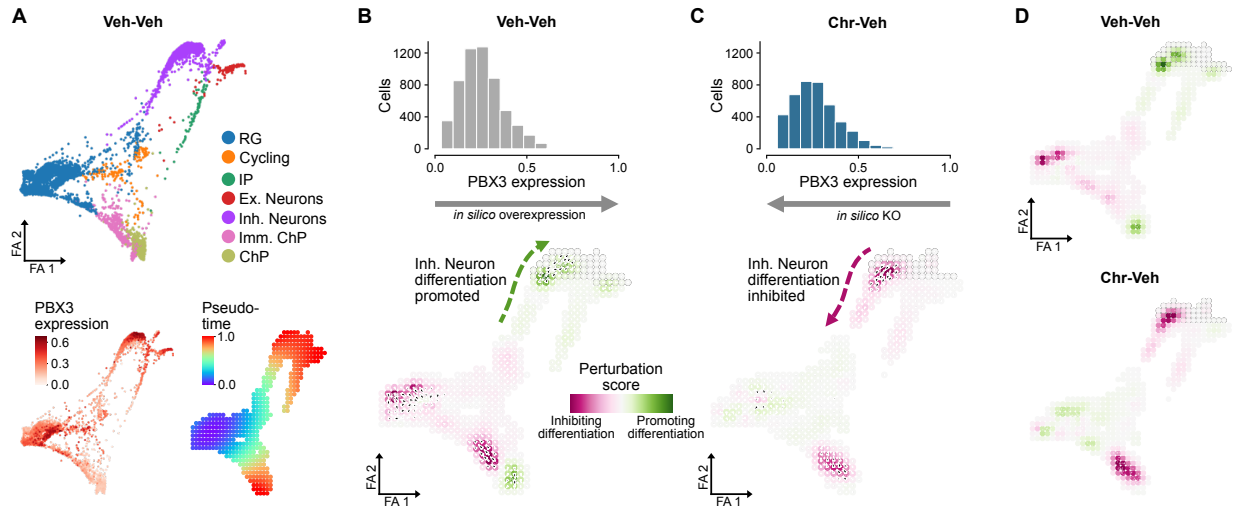


Fig. S5: Analyses of multi-modal gene regulatory networks associate *PBX3* with the regulation of inhibitory neuron priming in organoids from Line 409b2. (A) Force-directed graph layout of Line 409b2 Veh-Veh data. Top: colored by cell type. Bottom-left: colored by KNN-smoothed expression of *PBX3*. Bottom-right: Palantir pseudo-time discretized to a grid. FA, force-directed graph embedding. (B) Top: KNN-smoothed expression histogram of *PBX3* in Line 409b2 Veh-Veh data. Bottom: *PBX3* overexpression simulation vector field from Line 409b2 Veh-Veh data colored by perturbation scores. (C) Top: KNN-smoothed expression histogram of *PBX3* in Line 409b2 Chr-Veh data. Bottom: *PBX3* knockout (KO) simulation vector field from Line 409b2 Chr-Veh data colored by perturbation scores. (D) GRN perturbation simulation vector fields computed using the CellOracle(54) pre-built human promoter base-GRN colored by perturbation scores. Top: Line 409b2 Veh-Veh data with *PBX3* *in silico* overexpression. Bottom: Line 409b2 Chr-Veh data with *in silico* *PBX3* KO.

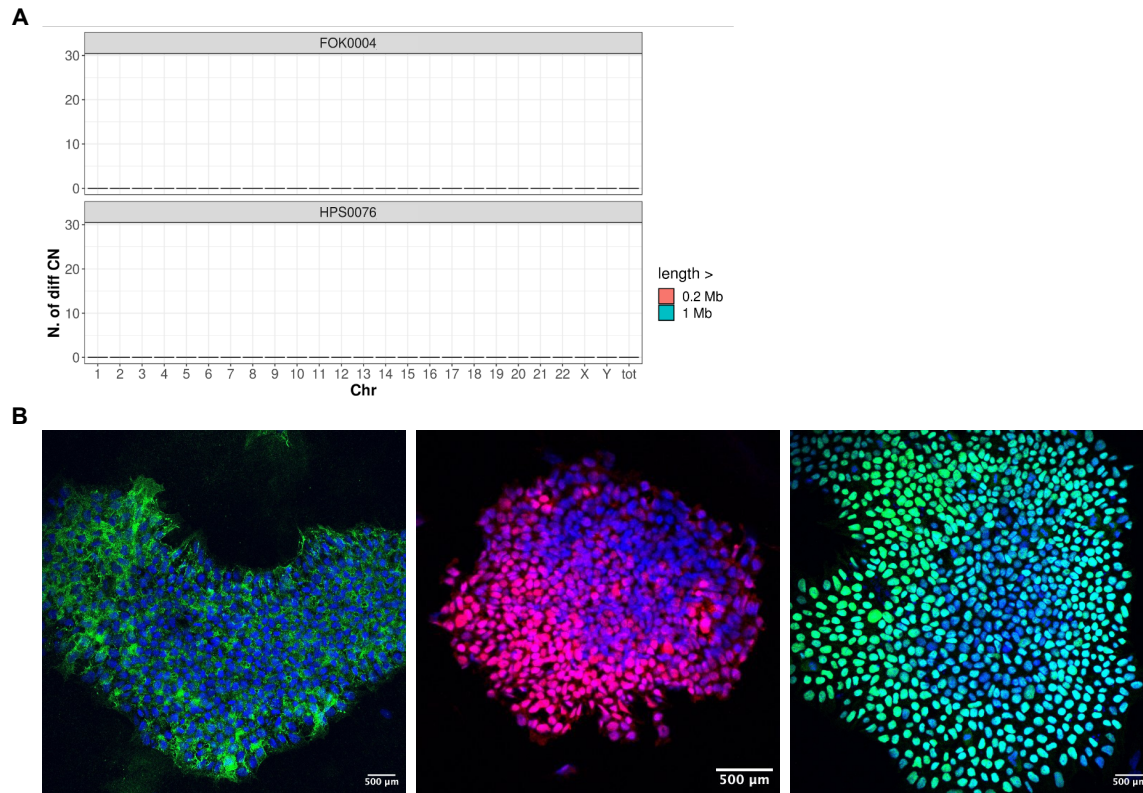


Fig. S6: Source iPSC line quality control. (A) Pairwise copy number variation (CNV) analyses using the Infinium GSA Array (Illumina), comparing the iPSC genome-wide genotypes at the organoid starting passage to the original donor sample. No CNV-level chromosomal abnormalities were detected for Line FOK4 (top) and Line 409b2 (bottom). **(B)** Immunofluorescence staining representing hiPSC quality control markers TRA-160 (left, green), OCT4 (middle, magenta), and NANOG (right, green), in Line FOK4.

Supplementary Data Tables (Separate Files).

Table S1. Differential expression results for the D70 Chr effect.

Table S2. GO-BP functional enrichment results for the D70 Chr significant DE genes.

Table S3. Differential expression results for the D90 Chr effect.

Table S4. Differential expression results for the D90 Acu effect.

Table S5. Differential expression results for the D90 Int effect.

Table S6. Lineage driver lists.

Table S7. IHC cell counting results.

Table S8. TF-target enrichment results for the D70 Chr significant DE genes.

Table S9. Pando GRN modules.